Temperature Coefficients of Transverse Elastic Properties of Scandium-Doped Aluminum Nitride (ScAlN) Thin Film Grown on Preformed Cavities

Sagnik Ghosh[1], Prakasha Chigahalli Ramegowda[1], Duan Jian Goh[1], Jaibir Sharma[1], Yul Koh[1], Joshua Lee[1†]

[1]Institute of Microelectronics (IME), Agency for Science, Technology and Research (A*STAR), 2 Fusionopolis Way, Innovis #10-20, Singapore, 138634, Republic of Singapore

[†]Currently at University of Technology Sydney, Australia

Email: Sagnik_Ghosh@ime.a-star.edu.sg

***Abstract*—This report presents a fully coupled method to extract the temperature coefficients (TCs) of transverse elastic properties for 15% scandium (Sc)-doped aluminum nitride (AlN) thin film from resonant test structures. The ScAlN thin film here is only 0.3µm-thick, grown on pre-formed cavities embedded below 2µm-thick silicon (Si) membranes with a 0.2µm-thick molybdenum (Mo) electrode over ScAlN. The intended parameters are extracted by interacting between finite element model methods and electrical measurement data of fabricated resonators. The proposed method allows extraction of first and second order TCs for transverse elastic properties. By extracting elastic properties at each temperature point, we directly obtain individual elastic property dependence on temperature without having any prior assumptions on the polynomial order of this dependence. This study marks one of the first reports on TCs for transverse elastic properties of ScAlN thin film: in-plane Young's modulus, in-plane shear modulus and in-plane Poisson's ratio.**

Keywords—Thin film ScAlN-on-silicon, Transverse elastic properties, temperature coefficients of elastic properties

I. INTRODUCTION

Scandium-doped aluminum nitride (ScAlN) films are promising for radio-frequency (RF) communication [1] and ultrasound devices, such as piezoelectric micromachined ultrasonic transducers (PMUTs) [2] due to their higher piezoelectric coefficient ($e_{31,f}$) as compared to pure AlN films. 15% Sc-doping has shown to enhance $e_{31,f}$ by 30% as compared to pure AlN films [3]. Ideally, RF communication devices and PMUTs are operated at their respective resonant frequencies. As such, there is a need to reduce the frequency variation with temperature to maintain a stable operation of such devices across a wide temperature range (industrial range: -40°C – 85°C). While the frequency stability with temperature variation is determined by the temperature coefficient of frequency (TCf), engineering the TCf of the devices requires the determination of temperature coefficient of elastic modulus (TCE). To date, 1st order temperature coefficient (TC) of a stiffness matrix element (c_{33}) for ScAlN film has been reported for thick ScAlN (≥ 4µm) film stacked between thinner top and bottom metal electrodes for film bulk acoustic resonator (FBAR) [4]. In the case of BAW resonators, FBARs, and high-overtone BARs (HBARs), c_{33} is particularly relevant for the resonant frequency of the thickness extensional mode used in these devices. In contrast, laterally vibrating contour mode resonators and various transverse mode resonators (e.g. PMUTs) have resonant frequencies dependent on the transverse elastic properties (Young's modulus, shear modulus and Poisson's ratio). There are reports of transverse elastic properties for ScAlN film (> 1µm) stacked between relatively thinner metal electrodes, where the frequency response is dominated by the properties of ScAlN film due to larger thickness ratio between ScAlN film and metal electrodes [5]. But the TCs of transverse elastic modulus are not known. Recently, having a thinner ScAlN film (< 0.4µm) on a degenerately doped silicon (Si) device layer (~2µm) has been shown to substantially reduce the TCf of the device [6]. The same process platform was used to demonstrate PMUTs [7] and laterally vibrating contour mode device [8]. Given that the elastic properties vary with Sc concentrations and film thickness, TCE of such thinner ScAlN films may well differ from the thicker films reported to date. Moreover, the frequency response of such piezoelectric-on-silicon devices are dominated by properties of thicker doped-Si with notably reduced influence from the properties of thinner ScAlN film. We herein extract the TCs for transverse elastic properties of 15% Sc-doped AlN thin film over a thicker doped-Si using a fully coupled method employing finite element (FE) simulation and measurement results.

II. METHOD OF PAREMETER EXTRACTION

First, we identify and initialize a set of unknown material parameters (to be extracted) in the FE model. Next, we simulate sensitivity of the resonant frequency to the respective material parameters to be extracted. Here, sensitivity measures the dependence of the resonant frequency on a given individual unknown material parameter. The respective sensitivity values inform the suitability of chosen resonant modes for extracting the full range of material parameters of interest. In each iteration, FE simulated and measured resonant frequencies are compared to obtain a new set of material parameters which are used to initialize the properties for the next iteration. This iterative

This research work was supported by A*STAR under "Nanosystems at the Edge" programme (Grant number: A18A4b0055).

analysis continues until the FE simulated and measured resonant frequencies finally converge using a gradient descent method.

A. Material properties to be extracted

In this study, we have used the compliance matrix of ScAlN, which has a hexagonal crystal structure with transverse isotropy and 5 independent elements (s_{11}, s_{12}, s_{13}, s_{33} and s_{44}) [9]:

$$\begin{bmatrix}\epsilon_1\\ \epsilon_2\\ \epsilon_3\\ \epsilon_4\\ \epsilon_5\\ \epsilon_6\end{bmatrix} = \begin{bmatrix} s_{11} & s_{12} & s_{13} & 0 & 0 & 0\\ s_{12} & s_{11} & s_{13} & 0 & 0 & 0\\ s_{13} & s_{13} & s_{33} & 0 & 0 & 0\\ 0 & 0 & 0 & s_{44} & 0 & 0\\ 0 & 0 & 0 & 0 & s_{44} & 0\\ 0 & 0 & 0 & 0 & 0 & 2(s_{11}-s_{12}) \end{bmatrix} \begin{bmatrix}\sigma_1\\ \sigma_2\\ \sigma_3\\ \sigma_4\\ \sigma_5\\ \sigma_6\end{bmatrix} \quad (1)$$

where ϵ_n and σ_n represents the respective strain and stress with n being the subscript, 1-6. The transverse elastic properties of ScAlN thin film include the in-plane Young's modulus (E_x), in-plane shear modulus (G_{xy}) and in-plane Poisson's ratio (ν_{xy}), which can be defined as functions of simply s_{11} and s_{12}:

$$E_x = \frac{1}{s_{11}} \quad (2)$$

$$G_{xy} = \frac{1}{2(s_{11}-s_{12})} \quad (3)$$

$$\nu_{xy} = -\frac{s_{12}}{s_{11}} \quad (4)$$

B. Sensitivity analysis for selection of MEMS resonators

The resonators used in this study were fabricated using a piezoelectric over silicon-on-nothing (PSON) process [8] where 15% Sc-doped AlN ($Sc_{0.15}Al_{0.85}N$) thin film was stacked between a bottom electrode formed by degenerately doped-Si (doping level > 3×10^{20} cm^{-3}) and a top electrode formed by molybdenum (Mo). A thin film of AlN passivates the top electrode. Thicknesses of respective layers for the FE model were obtained from cross-sectional analysis of fabricated devices as in [6].

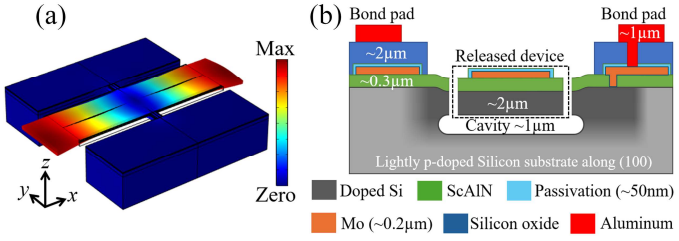

Fig. 1. (a) Finite element simulated displacement contour related to the length extensional (LE) vibration mode. (b) Cross-sectional schematic showing the vertical stack of the device.

The mechanical resonant frequency (f_n) has a direct dependence on the compliance parameter:

$$f_n = \frac{1}{\lambda\sqrt{s^E \rho^E}} \quad (5)$$

Here, λ is the corresponding wavelength, s^E and ρ^E denote the respective effective elastic compliance coefficient and effective density of the vertical stack forming the device. A sensitivity analysis was performed in COMSOL to select suitable MEMS resonators for the extraction of s_{11} and s_{12}. In the FE model, the properties of doped-Si were extrapolated from [10].

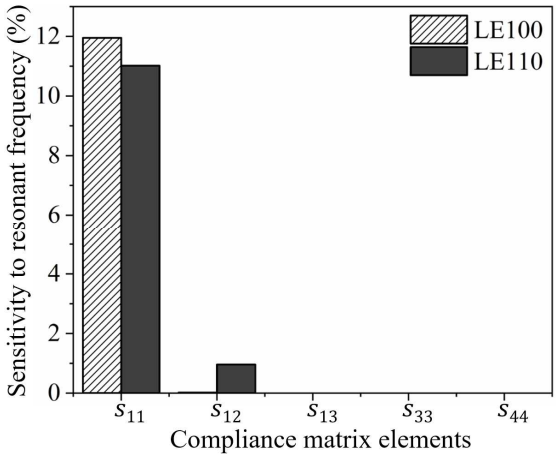

Fig. 2. FE simulated sensitivities of mechanical resonant frequency (f_n) with respect to each element of the compliance matrix (s_{11}, s_{12}, s_{13}, s_{33} and s_{44}) for LE mode devices aligned to <100> crystal axis (LE100) and <110> crystal axis (LE110) of Si within the (100) plane.

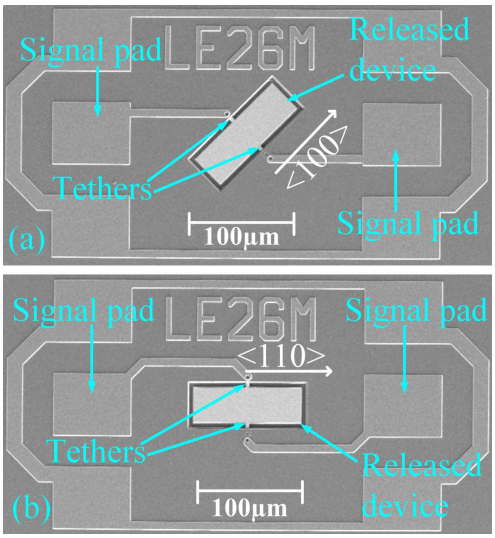

Fig. 3. Top-view scanning electron micrographs showing LE mode devices aligned to (a) <100> crystal axis and (b) <110> crystal axis of Si within the (100) plane.

Under sensitivity analysis, every compliance matrix element of ScAlN layer is individually varied to obtain the dependence of f_n to each respective compliance matrix element. While the initial values for the compliance matrix of ScAlN layer were extrapolated from AlN properties [11], the coefficient of thermal expansion (CTE) of 4.8ppm/°C [12], density of 3273kg/m^3 [13] and a measured permittivity of 14.31 were preset for the ScAlN layer in the FE model. We simulated length extensional (LE) mode resonators of the same dimensions, with one aligned to the <100> crystal axis (LE100) and another to the <110> crystal axis (LE110) of Si within the (100) plane using a parametric eigenfrequency analysis in COMSOL to obtain the sensitivities for f_n to the respective compliance matrix elements. Figure 1a

shows the displacement contour related to the LE mode shape, while Fig. 1b shows a cross-sectional view of the respective layers forming the vertical stack of the device. Fig. 2 shows the sensitivities of independent compliance matrix elements to f_n for both devices. Sensitivities below 0.1% were omitted in this study. As seen from Fig. 2, given the close to sole dependence on s_{11} for the LE100 device, the LE100 device was chosen to extract s_{11} of ScAlN. Next, the value for s_{11} was preset in the ScAlN layer for the LE110 device to extract s_{12}. Fig. 3 shows top-view scanning electron micrographs for both the LE100 (Fig. 3a) and LE110 (Fig. 3b) resonators. The resonator body for both structures are formed by a rectangular plate of 90µm×31µm, which is supported by two tethers along the mid-length where the nodes are found (Fig. 1a).

III. Extraction of Temperature Coefficients

We measured frequency responses for both LE100 and LE110 devices under varying temperature (-20°C to 60°C) inside a probe station using a network analyzer. The frequency response at each temperature point was fitted with a Butterworth-Van-Dyke (BVD) model to obtain f_n at individual temperature points. To extract TCs, respective elastic properties were obtained from f_n at each temperature. In this section, we first describe the extraction of s_{11} (and thereby E_x) from LE100, followed by the extraction of s_{11}, s_{12} from LE110.

A. Extraction of TCs for in-plane Young's modulus

Fig. 4a shows the measured admittance for LE100 at a temperature (T) of 25°C and fitted BVD model to obtain an f_n of 39.05MHz. Fig. 4b depicts a temperature dependence of -433Hz/°C on the extracted f_n, with a reduced first order TCF (TCf_1) of -11ppm/°C indicative of degenerate doping of Si.

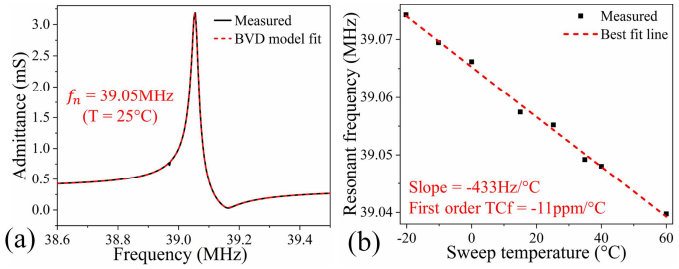

Fig. 4. (a) Measured admittance at a temperature (T) of 25°C and fitted BVD model to extract f_n of 39.05MHz for LE100. (b) Extracted values for f_n with varying temperature showing a temperature dependence of -433Hz/°C for LE100.

We used eigenfrequency analysis in COMSOL to obtain f_n at each temperature point used in the measurements. To consider thermal expansion and contraction with varying temperature, CTE was added for each material layer within the vertical stack of the FE model. The material extraction method was applied to value f_n to extract s_{11} at each individual temperature point. The extracted s_{11} at each temperature point was then inverted according to equation (2) to obtain the respective value of E_x. It is worth noting that the normalized shift for an elastic modulus (E) under varying temperature can be defined by a second order polynomial [10]:

$$\frac{\Delta E}{E_0} = \frac{E_T - E_0}{E_0} = TC_1(T - T_0) + TC_2(T - T_0)^2 \quad (6)$$

Here, T_0 refers to 25°C, T refers to individual temperature value, E_0 denotes the value of the elastic modulus at $T = T_0$, and E_T denotes the value of the elastic modulus at respective temperature points. TC_1 and TC_2 are the respective first and second order TCs for the elastic modulus. Fig. 5 shows the temperature dependent normalized shifts in extracted s_{11} (Fig. 5a) and E_x (Fig. 5b) fitted with a second order polynomial, as in equation (6), to obtain TC_1 and TC_2 which are summarized in Table 1.

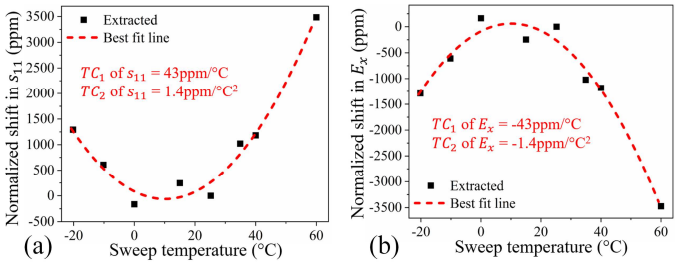

Fig. 5. Temperature dependent normalized shifts in the extracted values for (a) s_{11} and (b) E_x fitted with second order polynomials to obtain TC_1 and TC_2.

B. Extraction of TCs for in-plane shear modulus and Poisson's ratio

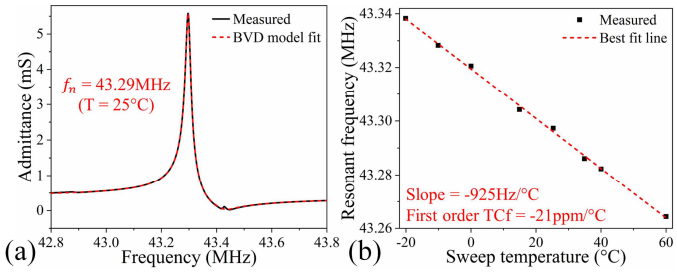

Fig. 6. (a) Measured admittance at a temperature (T) of 25°C and fitted BVD model to extract f_n of 43.29MHz for LE110. (b) Extracted values for f_n with varying temperature showing a temperature dependence of -925Hz/°C for LE110.

Similar to LE100, the measured frequency responses under varying temperature were fitted with a BVD model to obtain f_n at respective temperature points for LE110. Fig. 6a shows the measured admittance of LE110 at a temperature (T) of 25°C fitted with a BVD model to obtain an f_n of 43.29MHz. Fig. 6b depicts a temperature dependence of -925Hz/°C on the extracted f_n, with TCf_1 of -21ppm/°C. The higher TCf_1 in LE110 compared to the TCf_1 of LE100 can be attributed to differences in TCEs along the two crystal axes within the (100) plane [14].

In COMSOL, the value of s_{11} for ScAlN was parameterized with TC_1 and TC_2 values for s_{11} from Table 1 and with temperature as a variable according to equation (6). The same material extraction method was applied on LE110 to obtain s_{12} at respective temperature points. Fig. 7 shows the normalized shift in extracted values for s_{12} under varying temperature fitted with a second order polynomial to obtain TC_1 and TC_2 values for s_{12} as summarized in Table 1.

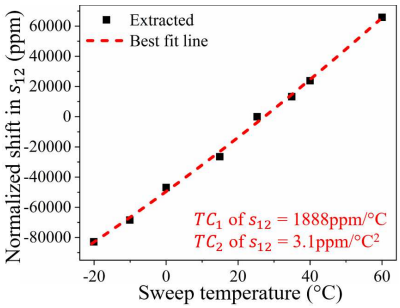

Fig. 7. Temperature dependent normalized shifts in the extracted values for s_{12} fitted with a second order polynomial to obtain TC_1 and TC_2.

Next, s_{12} for ScAlN was parameterized using the obtained TC_1 and TC_2 in accordance to equation (6). The consecutive parameterized forms of s_{11} and s_{12} were used to extract the temperature dependent variation of G_{xy} and ν_{xy}, in accordance to equations (3) and (4). As shown in Figs 8a and 8b, the dependence of normalized shifts in G_{xy} and ν_{xy} were individually fitted with a second order polynomial to obtain respective TC_1 and TC_2 values, which are summarized in Table 1.

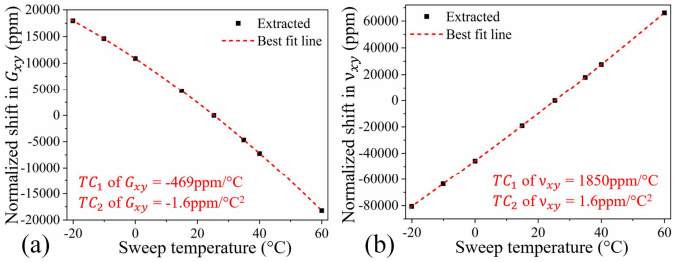

Fig. 8. Temperature dependent normalized shifts in the extracted values for (a) G_{xy} and (b) ν_{xy} fitted with second order polynomials to obtain TC_1 and TC_2.

IV. Discussions

The extracted material parameters were verified with measurement results from other resonators fabricated on the same PSON process. An average difference of < 1.8% between the measured and simulated results can possibly be due to the variation in thickness and doping level of Si across the wafer. In our model, the properties for doped-Si and thicknesses of the various layers were fixed based on the values from one site on the wafer. In reality, the extracted properties for ScAlN thin film are dependent on the extrapolated material parameters of doped-Si, and tied to the doping level (> 3×10^{20}cm^{-3}). The extraction method presented herein can be applied to obtain the values of transverse elastic properties and their associated TCs for different Sc concentrations and film thicknesses to facilitate the design and engineering of temperature stable resonators.

TABLE I. Summary of Extracted Temperature Dependent Properties for $Sc_{0.15}Al_{0.85}N$ Thin Film

Parameters	*Unit*	*Value at T = 25°C*	*TC_1 (ppm/°C)*	*TC_2 (ppm/°C²)*
s_{11}	1/Pa	4.09×10^{-12}	43	1.4
s_{12}	1/Pa	-1.23×10^{-12}	1888	3.1
E_x	GPa	244	-43	-1.4
G_{xy}	GPa	94	-469	-1.6
ν_{xy}	-	0.3	1850	1.6

Acknowledgment

This research work was supported by the Agency of Science, Technology and Research (A*STAR) under "Nanosystems at the Edge" programme (Grant number: A18A4b0055).

References

[1] Y. Zhu *et al.*, "ScAlN-based LCAT mode resonators above 2 GHz with high FOM and reduced fabrication complexity," IEEE Electron device Lett., vol. 38, pp. 1481-1484, October 2017.

[2] Y. Kusano *et al.*, "High-SPL air-coupled piezoelectric micromachined ultrasonic transducers based on 36% ScAlN thin-film," IEEE Trans. Ultrason., Ferroelect., Freq. Control, vol. 66, pp. 1488-1496, September 2019.

[3] M. Akiyama *et al.*, "Influence of scandium concentration on power generation figure of merit of scandium aluminum nitride thin films," Appl. Phys. Lett., vol. 102, pp. 021915, January 2013.

[4] T. Yanagitani *et al.*, "Electromechanical coupling and gigahertz elastic properties of ScAlN films near phase boundary," Appl. Phys. Lett., vol. 105, pp. 122907, September 2014.

[5] F. Parsapour *et al.*, "Material parameter extraction for complex AlScN thin film using dual mode resonators in combination with advanced microstructural analysis and finite element modeling," Adv. Electron. Mater., vol. 5, pp. 1800776, March 2019.

[6] S. Ghosh *et al.*, "Reduced TCF, high frequency, piezoelectric contour-mode resonators with silicon-on-nothing," Digests IEEE Ultrasonics Symposium, pp. 1-4, 2021.

[7] D. S. W. Choong *et al.*, "Silicon-on-nothing ScAlN pMUTs," Digests IEEE Ultrasonics Symposium, pp. 1-4, 2021.

[8] J. Sharma *et al.*, "Piezoelectric over silicon-on-nothing (pSON) process," Digests IEEE Ultrasonics Symposium, pp. 1-4, 2021.

[9] J. D. Larson *et al.*, "A BAW antenna duplexer for the 1900 MHz PCS band," Digests IEEE Ultrasonics Symposium, pp. 887-890, 1999.

[10] E. J. Ng *et al.*, "Temperature dependence of the elastic constants of doped silicon," IEEE J. Microelectromech. Syst., vol. 24, pp. 730–741, June 2015.

[11] J. Bjurstrom *et al.*, "Temperature compensation of liquid FBAR sensors," J. Micromech. Microeng., vol. 17, pp. 651–658, February 2007.

[12] Y. Lu *et al.*, "Elastic modulus and coefficient of thermal expension of piezoelectric $Al_{1-x}Sc_xN$ (up to x = 0.41) thin films," APL Mater., vol. 6, pp. 076105, July 2018.

[13] N. Kurz *et al.*, "Experimental determination of the electro-acoustic properties of thin film AlScN using surface acoustic wave resonators," J. App. Phys., vol. 126, pp. 075106, August 2019.

[14] H. Zhu *et al.*, "Crystallographic and eigenmode dependence of TCF for single crystal silicon contour mode resonators," Digests IEEE Micro Electro Mechanical Systems, pp. 761-764, 2013.